Journal of Applied Mechanics and Technical Physics, Vol. 45, No. 3, pp. 358–366, 2004

COMPUTATIONS OF INTERACTION OF AN INCIDENT OBLIQUE SHOCK WAVE WITH A TURBULENT BOUNDARY LAYER ON A FLAT PLATE

N. N. Fedorova and I. A. Fedorchenko

UDC 532.517.2:532.533.601.155

Results of numerical simulation of interaction between an oblique shock wave and a turbulent boundary layer formed in a supersonic (Mach number $M = 5$*) flow past a flat plate are presented. The computations are performed for three cases of interaction of different intensity, which result in an attached or detached flow. Numerical results are compared with experimental data. The effect of flow turbulence and shock-wave unsteadiness on flow parameters is studied.*

Key words: *shock wave, boundary layer, separated flow, turbulence, heat transfer.*

Along with the physical experiment, mathematical simulation plays an important role in studying high-velocity turbulent flows for design of supersonic and hypersonic flying vehicles and developing methods for flow control. Shock wave–boundary layer interaction has been extensively studied [1–5]. It is known that dynamic and thermal loads due to such an interaction are usually critical for the flying vehicle. At the same time, the structure of the resultant flow is rather simple, which makes it possible to analyze its specific features and evaluate the possibility of using the turbulence model and numerical algorithm for predicting the expected loads.

The flow structure in the interaction region significantly depends on the flow regime in the boundary layer and shock-wave intensity and angle of incidence [1]. Depending on the interaction intensity and shock-wave incidence angle, either regular or irregular reflection can occur. Irregular reflection is observed at moderate supersonic velocities and high angles of shock incidence. A reflected shock with a straight-line segment arises near the boundary layer. If the incident shock-wave intensity is small, reflection occurs without boundary-layer separation. An increase in shock-wave intensity leads to a transonic configuration of interaction with a λ-structure formed at the base of the incident shock wave [1]. In addition, several types of shock wave–boundary layer interaction are possible, leading to different types of reflected waves [6].

If the incident shock intensity is rather high, a separation region can be formed; a laminar boundary layer separates at a lower threshold pressure. In the case of a turbulent boundary layer, the separation-region length is commensurable with the undisturbed boundary-layer thickness, and the separation-region thickness is much smaller than the latter.

In considering turbulent separation, special attention is paid to mechanisms of flow separation and reattachment in regions of shock wave–boundary layer interaction and to the effect of the Reynolds and Mach numbers on parameters of these regions.

It was shown [7] that a particular angle of the incident shock wave that gives rise to flow separation corresponds to each value of the Mach number. This is confirmed by studying shock wave–boundary layer interaction in supersonic diffusers.

Interaction of a turbulent boundary layer with a compression wave was experimentally studied in [8, 9] for a Mach number $M = 2.9$ and Reynolds numbers $Re = (2.2–5.9) \cdot 10^4$.

Results of experimental studies of interaction of an incident oblique shock generated by an 8° wedge with the boundary layer for $M = 2.3$ and $Re_\delta = 6 \cdot 10^4$ are described in [10, 11].

Institute of Theoretical and Applied Mechanics, Siberian Division, Russian Academy of Sciences, Novosibirsk 630090. Translated from Prikladnaya Mekhanika i Tekhnicheskaya Fizika, Vol. 45, No. 3, pp. 61–71, May–June, 2004. Original article submitted March 28, 2003; revision submitted May 8, 2003.

 0021-8944/04/4503-0358

Interaction of a turbulent boundary layer with an incident shock wave generated by a flat wedge whose angle could be varied was considered in the experiment of [12]. The dependences of the separation-region length on the shock-wave incidence angle for M = 2.96 are given. As the shock-generator angle increases, the shock intensity also increases, disturbances propagate to a greater distance, and the separation point is shifted upstream. The separation-region size also depends on the Reynolds number. At high values of Reynolds number, the shock-generator angle corresponding to incipient separation increases with increasing Reynolds number for all Mach numbers considered [12], and the opposite tendency is observed for comparatively low values of Re [2].

The influence of the free-stream Mach number on the character of three-dimensional interaction of a shock wave and a turbulent boundary layer was considered experimentally and theoretically in [13]. The angle of the shock generator varied from 4 to 22°, M = 2–4, and $\mathrm{Re}_1 = (50\text{–}80) \cdot 10^6$ m^{-1}. It was found [13] that the flow parameters in the interaction region depend on the flow Mach number and shock-wave intensity. The agreement between the computations and experiments worsens with increasing interaction intensity.

The parameters of the separation region on a flat wall of a rectangular-section nozzle for M = 2.9 and $\mathrm{Re}_\delta = 9.73 \cdot 10^5$ under adiabatic wall conditions were experimentally studied in [14]. Data on static pressure distributions on the plate surface for attached flows and for flows with separation are presented. The measurement results are in agreement with experimental data of other authors.

Experimental results for M = 1.30–1.42 are described in [15]. For different shock intensities, events with incipient separation, developed separation region, and large separation bubble are considered. The measurements show that a high level of turbulence affecting flow parameters is generated in the first phase of interaction corresponding to intense deceleration. Therefore, the neglect of normal components in impulse and turbulent energy equations is invalid in the region of the shock-wave base, where the flow experiences significant deceleration. It was found that the boundary layer is significantly nonequilibrium in the course of interaction. Since the lifetime of large structures formed in the zone of intense turbulence is rather long, relaxation of a new state of equilibrium further downstream is a long process.

The normal and tangential components of the Reynolds stresses for M = 2.9 in the case of an adiabatic wall were measured in [16]. It was shown that the normal components of the Reynolds stresses are rather low in the entire flow region, and the gradients of tangential components of stresses in the interaction region are small as compared to the pressure gradient.

An important issue of shock wave–boundary layer interaction is heat transfer [17]. In the case of shock-wave incidence onto the surface and separation incipience, the heat-flux distribution on the surface can become significantly nonuniform. Heat-flux peaks are of significant danger for the vehicle structure, and it is important to accurately predict them for practical applications.

Experimental results for M = 4, $\mathrm{Re} = (1.3\text{–}1.5) \cdot 10^7$, and $T_w/T_0 = 0.59\text{–}0.65$ (T_w is the wall temperature and T_0 is the free-stream total temperature) are presented in [18]. The shock-wave angle to the surface of a sharp flat plate where the measurements were performed varied from 17°8′ to 22°8′. The pressure and heat-flux distributions on the plate surface were considered.

Heat transfer on a flat plate in two- and three-dimensional interaction of an oblique shock wave and a boundary layer at M = 3 and 5 was considered in [19]. It was noted that the heat-flux peak increases with increasing shock-wave intensity. Based on the maximum pressure value, one can evaluate the maximum heat flux in the interaction region, using correlation analysis. Interaction of a streamwise oscillating shock wave with a laminar and turbulent boundary layer on a flat plate was considered in [20]. The experimental work [21] involved the study of typical features of the flow in the region of interaction of an oscillating shock wave with a boundary layer on the body surface; the parameters varied in the experiments were the frequency and amplitude of oscillations and the shock-wave intensity. The general features of the flow in the interaction region were revealed, and the dependences between the maximum values of pressure and heat fluxes in the interaction region were found. An analysis of the flow pattern in the region of unsteady interaction showed that the separation region for $\mathrm{Re} = 1.37 \cdot 10^6$ acquires a clear stable three-dimensional wavy structure similar to Taylor–Görtler vortices formed in the region of flow separation and reattachment in the turbulent regime. For an oscillation frequency of 10 Hz and an amplitude of $0.136x_0$ (x_0 is the distance from the leading edge of the plate to the interaction region), an increase in the Reynolds number from $1.37 \cdot 10^6$ to $2.11 \cdot 10^6$ decreases the scale of the structures being formed. A comparison of heat fluxes in the region of flow reattachment upon steady and unsteady interaction shows that the greater the shock-wave intensity, the greater the effect of its oscillations on heat-transfer intensity. This effect is particularly significant in the case of a turbulent boundary layer.

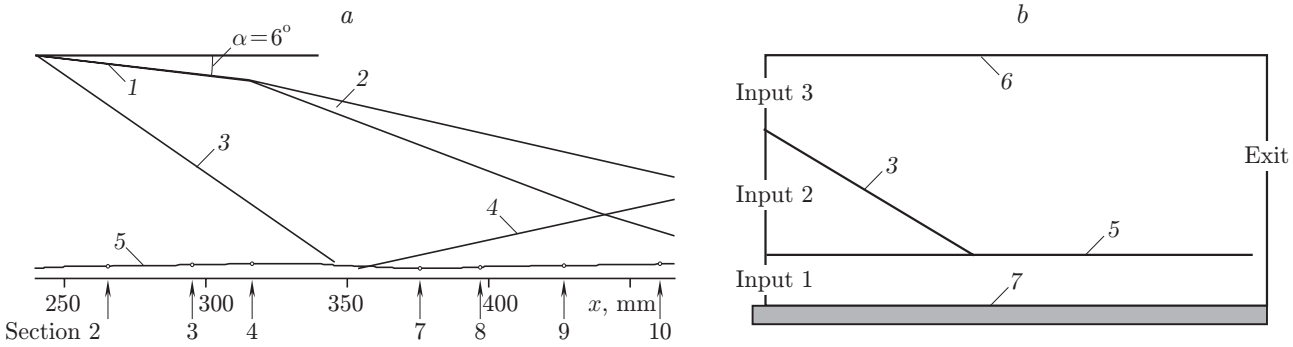

Fig. 1. Experimental flow pattern for $\alpha = 6^\circ$ (a) and schematic of the computational domain (b): 1) shock-wave generator; 2) expansion wave; 3) incident shock wave; 4) reflected shock wave; 5) boundary-layer edge; 6) upper boundary; 7) plate; the arrows indicate cross sections 2–4 and 7–10, where the profiles of mean parameters in the boundary layer were measured.

Results of numerical computations with the use of different mathematical models and semi-empirical models of turbulence were described in [22–25]. The results obtained by large eddy simulation were presented in [26]. The main attention was paid to reliability of predicting the flow structure, separation-region size, and dynamic and thermal loads that occur in such an interaction. It should be noted that the accuracy of computing the parameters of turbulent separated flows decreases with increasing interaction intensity. Therefore, it seems reasonable to simulate flows with sufficiently high Mach numbers.

The present paper describes computations for conditions of the experiment performed at the Institute of Fluid Mechanics DLR (Göttingen, Germany) [27, 28] in the Lüdwig tube for the following parameters: stagnation temperature $T_0 = 410$ K, stagnation pressure $P_0 = 2.12$ MPa, unit Reynolds number $\mathrm{Re}_1 = 40 \cdot 10^6$ m^{-1}, and wall temperature $T_w = (300 \pm 5)$ K. The shock wave was generated by a plate (shock generator) whose angle of inclination α determined the incident wave intensity. The free-stream Mach number was M = 5. The experiment was conducted for shock-wave generator angles $\alpha = 6$, 10, and 14° corresponding to an attached flow and to flows with local and large-scale separation regions.

The experimental data of [27] have been already used as a test case for verification of numerical algorithms within a European Space Agency/European Space Research and Technology Center project [29]. A comparison of results obtained by various computational codes developed at the Computational Aerodynamics Department of the Swedish Defence Research Agency (FFA, Sweden), Technical University in Munich (Germany), and Dassault Aviation (France) and different turbulence models showed that the best agreement with the experiment for the case of weak and moderate interaction is achieved by using the EARSM full explicit algebraic model of turbulence proposed in [29] and based on the Wilcox turbulence model [30].

Figure 1a shows the flow pattern for the case $\alpha = 6^\circ$, which was constructed on the basis of schlieren pictures, measured total and static pressures, and velocity profiles in cross sections 2–10. A detailed description of the experiment and results obtained can be found in [27, 31].

The computations were performed within the framework of the full Favre-averaged Navier–Stokes equations supplemented by the Wilcox two-parameter turbulence model [30]. The model and computation methods were described in [31, 32].

The computational domain was bounded by the upper, input, and output sections and by the plate and did not include the shock generator (Fig. 1b). The velocity, density, and temperature profiles in the input section 1 were determined by boundary-layer computations under the condition of matching of experimental and numerical values of integral boundary-layer characteristics and skin friction. Undisturbed flow conditions were imposed in the input section 2. In section 3, the conditions were found by solving an inviscid problem on an oblique shock wave:

$$\begin{aligned}
&\bar{u} = 0.983, \quad \bar{v} = -0.1, \quad \bar{\rho} = 1.66, \quad \bar{T} = 0.09 \quad \text{for} \quad \alpha = 6^\circ;\\
&\bar{u} = 0.95, \quad \bar{v} = -0.17, \quad \bar{\rho} = 2.1, \quad \bar{T} = 0.105 \quad \text{for} \quad \alpha = 10^\circ;\\
&\bar{u} = 0.91, \quad \bar{v} = -0.23, \quad \bar{\rho} = 2.63, \quad \bar{T} = 0.12 \quad \text{for} \quad \alpha = 14^\circ.
\end{aligned}$$

Here, $\bar{u} = u/U_\infty$, $\bar{v} = v/U_\infty$, $\bar{\rho} = \rho/\rho_\infty$, $\bar{T} = T/(c_v U_\infty^2)$, $\bar{p} = p/(\rho_\infty U_\infty^2)$, $c_v = 715$ J/(kg·K) is the air specific heat at constant volume, and $U_\infty = 825$ m/sec and $\rho_\infty = 0.215$ kg/m^3 are the free-stream velocity and density.

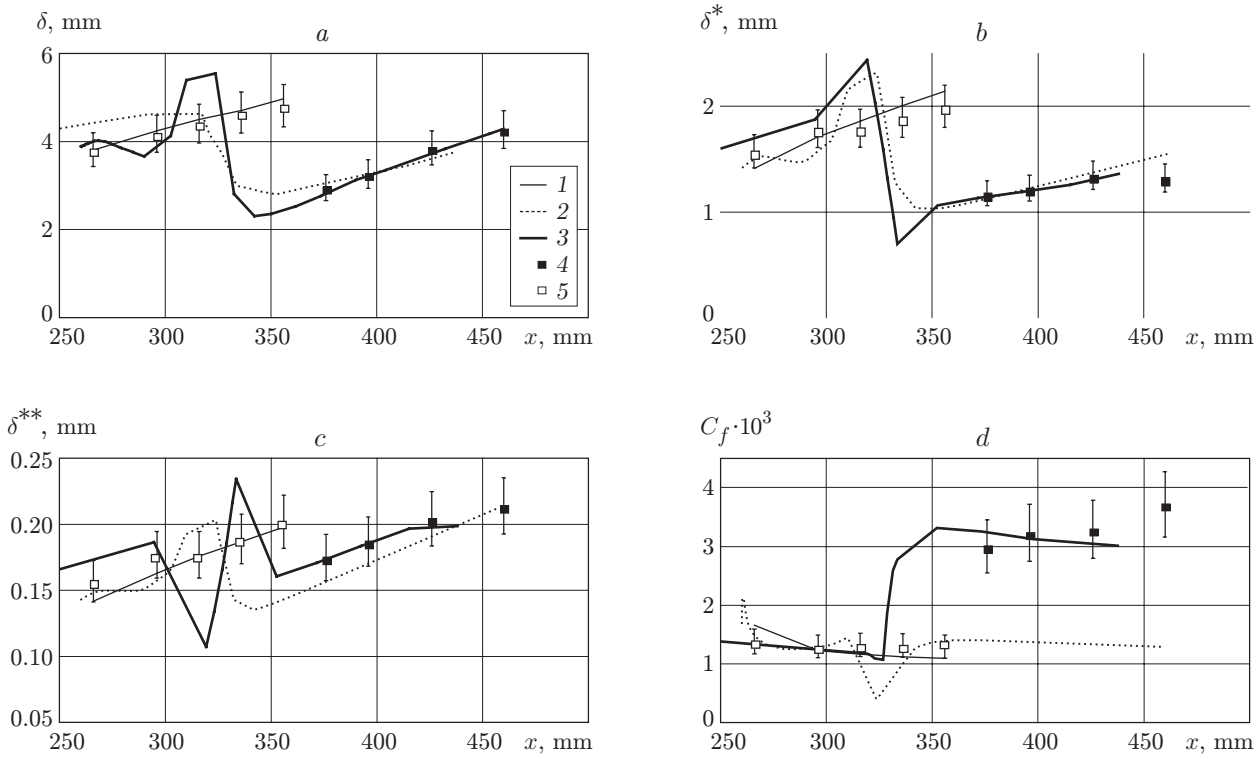

Fig. 2. Distributions of the boundary-layer parameters (a–c) and skin friction (d): curve 1 and points 5 refer to the undisturbed flow, curves 2 and 3 and points 4 refer to weak shock wave–boundary layer interaction ($\alpha = 6^\circ$); the computations were performed by the boundary-layer equations (curves 1 and 2) and full Navier–Stokes equations (curve 3); points 4 and 5 refer to the experimental data.

The conditions of the "simple" wave and the so-called "soft" conditions were imposed on the upper and right boundaries, respectively. The boundary conditions for velocity on the plate surface were the no-slip conditions. In accordance with test conditions, the wall temperature was assumed to be constant: $T = 300$ K. A rectangular regular grid refined toward the plate surface was used; in most cases, the grid had 200 nodes along the plate and 150 nodes in the direction normal to the plate surface.

The flow parameters in the input section were calculated by the boundary-layer equations. Within the framework of the same model, the boundary layer subjected to an external pressure gradient was calculated for the case of unseparated interaction ($\alpha = 6^\circ$). The pressure distributions for these computations were taken from the experiment. Figure 2 shows the experimental and computed distributions of boundary-layer parameters (δ, δ^*, and δ^{**}) and skin friction C_f for the undisturbed flow and for the case $\alpha = 6^\circ$. The turbulence model was identical in computations by the boundary-layer equations and full Navier–Stokes equations. An analysis of Fig. 2 shows that the integral thicknesses δ, δ^*, and δ^{**} calculated by the boundary-layer equations are in good agreement with the experimental values, but the skin friction behind the interaction point is significantly lower than the experimental value.

Figure 3 shows the schlieren pictures and computed density fields for three cases of interaction. The numerical and experimental data are in good agreement, namely, the positions of the incident and reflected shock waves and the λ-structure formed owing to separation, and also the separation-region size.

Figure 4 shows the experimental and numerical distributions of pressure, skin friction, and Stanton number for all cases of interaction. The open points in Fig. 4b refer to data obtained by velocity-profile measurements [27], and the filled points show data that were obtained by an optical method for skin-friction measurement [28]. The computed pressure distribution agrees with the experimental one in all cases of interaction. Reasonable agreement of skin-friction distributions for $\alpha = 6$ and 10° should also be noted.

A comparison of mean velocity, density, and temperature profiles for different wave intensities [31] shows that the experimental and numerical data are in good agreement in the case of weak and moderate interaction.

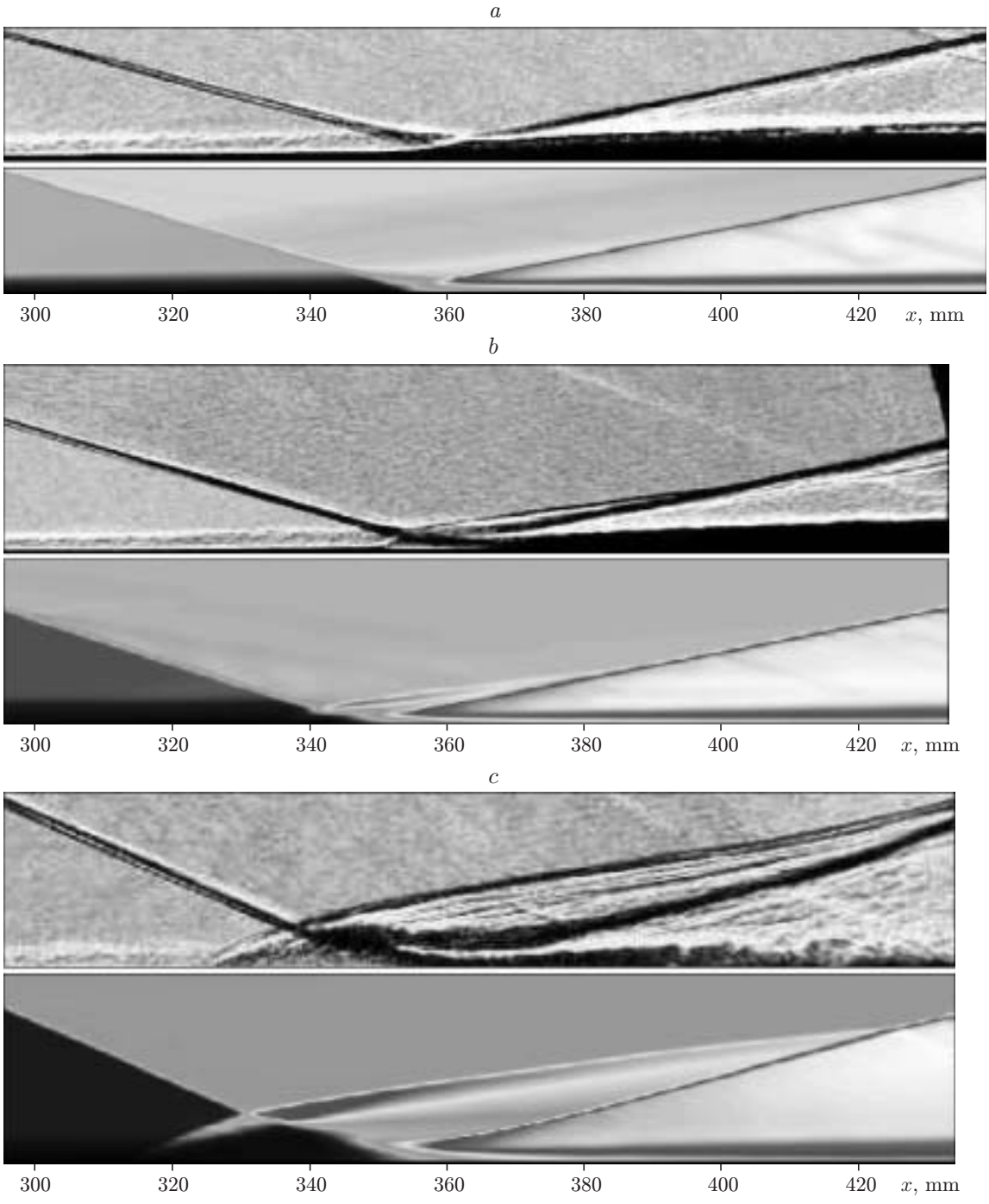

Fig. 3. Schlieren pictures of the flow (above) and computed density fields (below) for $\alpha = 6$ (a), 10 (b), and 14° (c).

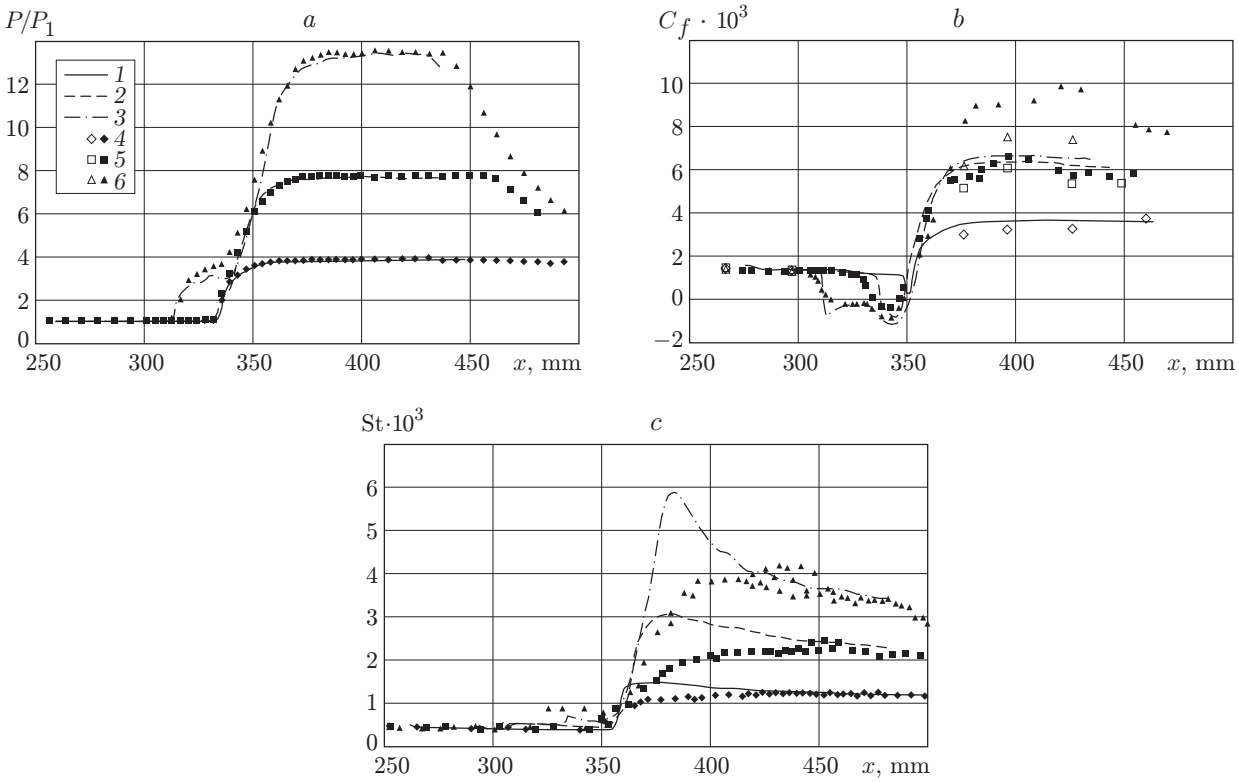

Fig. 4. Distributions of pressure (a), skin friction (b), and Stanton number (c) on the wall: the curves and points refer to the computations and experiment, respectively, for $\alpha = 6$ (1 and 4), 10 (2 and 5), and 14° (3 and 6).

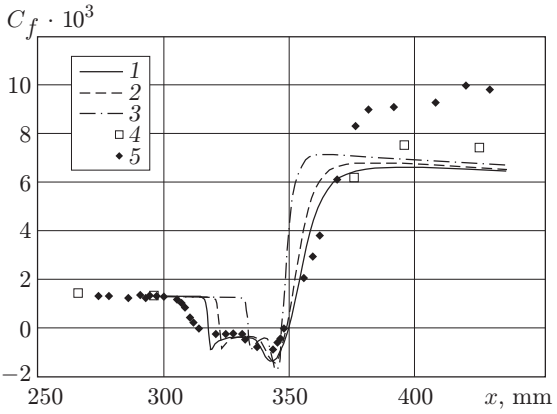

Fig. 5. Skin-friction distribution for different values of external turbulence ($\alpha = 14°$): the curves refer to the computations for $k_e = 10^{-3}$ (1), $2 \cdot 10^{-3}$ (2), and $4 \cdot 10^{-3}$ (3); points 4 and 5 show the experimental data obtained by different techniques.

The greatest difference in data, especially in the near-wall region, is observed for the most intense interaction. For $\alpha = 14°$, the computations underpredict the values of skin friction and boundary-layer thickness, which leads to significant differences in the profiles of mean gas-dynamic parameters, and overpredict the heat-flux values at the reattachment point.

A possible reason for this disagreement can be the failure of the turbulence model used to reliably predict turbulence generation due to interaction with strong shock waves. The properties of turbulence models in separated flows were considered in many papers (see, e.g., [22, 29, 30, 33]), where various modifications of existing models for improving the predictions of flow parameters were suggested. Note, no parametric study of turbulence models

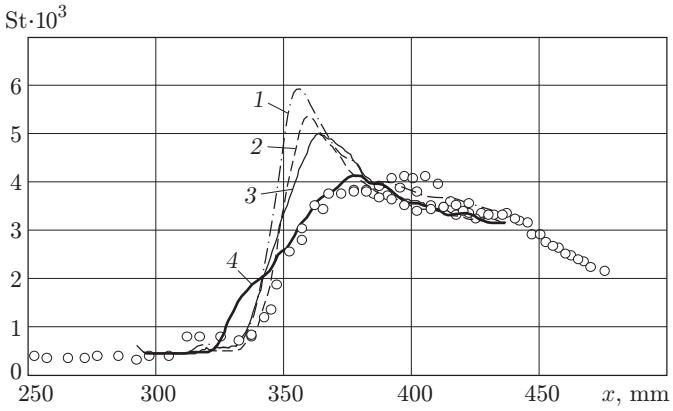

Fig. 6. Effect of oscillation amplitude on the Stanton number distribution for an oscillation frequency $f = 1000$ Hz: the curves show the computations for $A = 0$ (1), 0.5 (2), 1.1 (3), and 2.5 (4); the points show the experimental data.

was performed in the present work. Another possible reason for the difference in data can be the fact that the computations ignore some factors inherent in a real physical process, in particular, unsteadiness of the separation shock, external turbulence, and acoustic waves induced by the generator boundary layer in the zone of the laminar–turbulent transition. For the case $\alpha = 14°$, a series of parametric computations was performed to study the effect of external turbulence $k_e = \sum_i \langle u_i' u_i' \rangle / U_\infty^2$ and separation-shock unsteadiness on flow parameters. Figure 5 shows the skin-friction distributions for different k_e. The computations show that this parameter has a significant effect on the separation-region length and distribution of parameters in the interaction region. It follows from Fig. 5 that the separation-region size decreases with increasing k_e. The peak in the Stanton number distribution increases with increasing k_e, which can be attributed to enhanced heat transfer due to more intense turbulent mixing. The fullness of velocity profiles increases with increasing k_e. At the same time, variation of external turbulence does not produce any significant effect on skin friction and level of heat fluxes behind the reattachment point.

To study the effect of unsteadiness on flow parameters, we simulated the unsteady position of the separation shock by setting particular conditions in the input cross section of the computational domain. In the input sections 2 and 3 (see Fig. 1b), the shock position depended on time by the harmonic law

$$y = y_0 + A \sin(\pi f t + \pi/2),$$

where y_0 and y are the initial and current shock positions, A and f are the unsteadiness amplitude and frequency, and t is the current time.

We consider the case of the most intense interaction ($\alpha = 14°$). The computations were performed for different frequencies f and amplitudes A of shock oscillations. Figure 6 shows the period-averaged Stanton numbers for a fixed frequency $f = 1000$ Hz and different amplitudes A normalized to the boundary-layer thickness δ ahead of the interaction region. The peak in the heat-transfer distribution decreases with increasing amplitude. The effect of the shock-oscillation frequency f for a fixed value $A = 1.1$ is very small (Fig. 7).

Thus, interaction of an oblique shock wave with a turbulent boundary layer was numerically simulated for M = 5 for three cases of interaction of different intensity, including interaction with and without separation. The computations were performed within the framework of the full averaged Navier–Stokes equations supplemented by the Wilcox turbulence model. The flow without separation was also calculated by the boundary-layer equations.

The values calculated by the simplified boundary-layer model are in good agreement with the experimental values of integral boundary-layer characteristics, but the skin friction behind the reattachment point is substantially underpredicted in these computations.

The computations by the full model accurately predict the experimental flow pattern, separation-region size, and pressure distribution in all three cases considered. For weak and moderate-intensity interaction, the computations reliably predict the behavior of skin friction and heat fluxes, as well as mean velocity profiles. In the case of strong interaction, a discrepancy in numerical and experimental values of skin friction and boundary-layer thickness should be noted, which leads to significant differences in profiles of mean gas-dynamic parameters. In

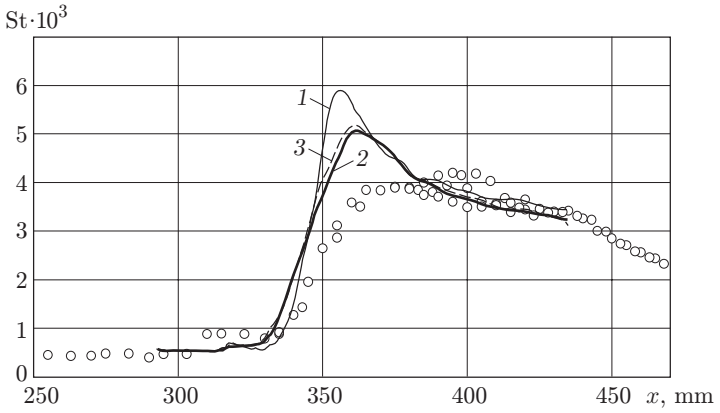

Fig. 7. Effect of oscillation frequency on the Stanton number distribution for an oscillation amplitude $A = 11$: the curves show the computations for $f = 0$ (1), 1000 (2), and 2000 Hz (3); the point show the experimental data.

addition, the computations significantly overpredict the heat fluxes at the reattachment point for moderate and strong interaction.

Possible reasons for the disagreement between the numerical and experimental results are considered. The effect of external turbulence and separation-shock unsteadiness on flow parameters is studied. If unsteadiness is taken into account, the peak in the Stanton number distribution decreases, which ensures reasonable agreement of the numerical and experimental data.

REFERENCES

1. L. V. Gogish and G. Yu. Stepanov, *Turbulent Separated Flows* [in Russian], Nauka, Moscow (1979).
2. P. Chang, *Separation of Flow*, Pergamon Press, Oxford (1970).
3. J. E. Greene, "Interaction between shock waves and turbulent boundary layers," *Progr. Aerospace Sci.*, **11**, 235–340 (1970).
4. J. Delery, "Shock wave/turbulent boundary layer interaction and its control," *Progr. Aerospace Sci.*, **22**, 209–280 (1985).
5. N. F. Krasnov, V. N. Koshevoi, and V. T. Kalugin, *Aerodynamics of Separated Flows* [in Russian], Vysshaya Shkola, Moscow (1988).
6. L. F. Henderson, "The reflection of a shock wave at a rigid wall in the presence of a boundary layer," *J. Fluid Mech.*, **30**, pt 4, 699–722 (1967).
7. Th. J. Nussdorfer, "Some observations of shock-induced turbulent separation on supersonic diffusers," NACA Res. Memorandum No. E51L26 (1954).
8. M. S. Holden, "Shock wave–boundary layer interaction in hypersonic flow," AIAA Paper No. 72-74 (1972).
9. W. L. Hankey and M. S. Holden, "Two-dimensional shock wave–boundary layer interactions in high speed flows," AGARD Report No. AG-203, Paris (1975).
10. J. Deleuze, "Structure d'une couchee limite turbulente soumise a une de choc incidente," Thes. ... Doct. Phys. Univ., Aix-Marseille (1995).
11. H. Laurent, "Turbulence d'une interaction onde de choc/couche limite sur une paroi adiabatique ou chauffee," Thes. ... Doct. Phys., Univ. Aix-Marseille (1996).
12. C. H. Low, "Supersonic shock wave–turbulent boundary layer interaction," *AIAA J.*, **14**, No. 6, 139–140 (1976).
13. F. K. Lu and G. S. Settles, "Mach number effects on conical surface features of swept shock boundary-layer interactions," AIAA Paper No. 1365 (1987).
14. D. C. Reda and J. D. Murphy, "Shock wave/turbulent boundary layer interactions in rectangular channels," *AIAA J.*, **11**, No. 2, 139–140 (1973).
15. J. M. Delery, "Experimental investigation of turbulence properties in transonic shock/boundary layer interactions," *AIAA J.*, **21**, No. 2, 180–185 (1983).

16. W. C. Rose and D. A. Johnson, "Turbulence in shock–wave boundary layer interaction," *AIAA J.*, **13**, No. 7, 884–889 (1975).
17. V. Ya. Borovoi, *Gas Flow and Heat Transfer in Shock Wave–Boundary Layer Interaction Regions* [in Russian], Mashinostroenie, Moscow (1983).
18. H. Masanori and S. Akira, "Measurements of heat-transfer coefficients in the interaction regions between oblique shock waves and turbulent boundary layers with a multi-layered thin film heat transfer gauge," *J. Jpn. Soc. Aeronaut. Space*, **35**, No. 397, 85–90 (1987).
19. I. A. Kondrat'ev, "Experimental study of heat transfer on a flat plate with oblique shock wave–laminar boundary layer interaction," *Uch. Zap. TsAGI*, **2**, No. 2, 18–23 (1971).
20. V. Ya. Neiland, O. I. Nosarev, V. S. Khlebnikov, and P. G. Tsyganov, "Investigation of interaction of a streamwise oscillating shock wave with a laminar boundary layer," *Tr. TsAGI*, No. 2456 (1989).
21. S. V. Kuimov and V. S. Khlebnikov, "Investigation of interaction of an unsteady shock wave with a boundary layer on a flat plate in the transitional regime," *Izv. Ross. Akad. Nauk, Mekh. Zhidk. Gaza*, No. 6, 174–180 (1992).
22. D. C. Wilcox, "Numerical study of separated turbulent flows," AIAA Paper No. 584 (1974).
23. A. N. Gil'manov, *Methods of Adaptive Grids in Gas-Dynamic Problems* [in Russian], Fizmatlit, Moscow (2000).
24. S. R. Chacravarthy and S. Osher, "Computing with high-resolution upwind schemes for hyperbolic equations," *Lecture Appl. Math.*, **22**, Part 1, 57–86 (1985).
25. A. I. Tolstykh, *Compact Difference Schemes and their Application to Aerohydrodynamic Problems* [in Russian], Nauka, Moscow (1990).
26. D. Knight, H. Yan, A. Panaras, and A. Zheltovodov, "RTO WG 10: CFD validation for shock wave turbulent boundary layer interactions," AIAA Paper No. 2002-0437 (2002).
27. E. Schülein, P. Krogmann, and E. Stanewsky, "Documentation of two-dimensional impinging shock/turbulent boundary layer interaction flow," Doc. DLR, No. IB 223-96, Rev. A 49, Göttingen (1996).
28. E. Schülein, S. Koch, and H. Rosemann, *Skin friction measurement and transition detection techniques for the Ludwieg-tubes at DLR,* in: *Proc. of the AGARD FDP Symp. on Advanced Aerodynamic Measurement Technology* (Seattle, USA, Sept. 22–25, 1997), AGARD, Neully-sur-Seine, France (1998), pp. 23-1–23-9.
29. I. A. A. Lindblad, S. Wallin, A. V. Johansson, et al., "A prediction method for high speed turbulent separated flows with experimental verification," AIAA Paper No. 98-2547 (1998).
30. D. C. Wilcox, "Reassessment of the scale determining equation for advanced turbulence models," *AIAA J.*, **32**, No. 11, 1299–1310 (1988).
31. N. N. Fedorova, I. A. Fedorchenko, and E. Shuelein, "Impinging shock wave/flat plate turbulent boundary layer interaction at M = 5 (experiments and computations)," in: *Proc. of the 10th Int. Conf. on the Methods of Aerophysical Research* (Novosibirsk–Tomsk, July 9–16, 2000), Part 1, Publ. House SB RAS, Novosibirsk (2000), pp. 71–78.
32. I. A. Bedarev, A. A. Maslov, A. A. Sidorenko, et al., "Experimental and numerical study of a hypersonic separated flow in the vicinity of a cone-flare model," *J. Appl. Mech. Tech. Phys.*, **43**, No. 6, 867–876 (2002).
33. G. Barakos and D. Drikakis, "Investigation of nonlinear eddy-viscosity turbulence models in shock/boundary layer interaction," *AIAA J.*, **38**, No. 3, 461–469 (2000).